One-particle two-time diffusion in three-dimensional homogeneous isotropic turbulence

D. R. Osborne[a)]
Space and Atmospheric Physics/Turbulence and Mixing Group, Imperial College London, Exhibition Road, London SW7 2BY, United Kingdom

J. C. Vassilicos[b)]
Turbulence and Mixing Group, Department of Aeronautics, Imperial College London, Exhibition Road, London SW7 2BY, United Kingdom

J. D. Haigh[c)]
Space and Atmospheric Physics, Department of Physics, Imperial College London, Exhibition Road, London SW7 2BY, United Kingdom

(Received 23 June 2004; accepted 1 December 2004; published online 28 January 2005)

A model of turbulence based on a summation of Fourier modes with an imposed turbulent energy spectrum, $E(k) \sim k^{-p}$, is used to investigate the characteristics of one-particle diffusion in turbulent flow. The model is described and the general Eulerian field is investigated. Using a number of Lagrangian statistical measures the results from the model are compared with laboratory experiments [N. Mordant, P. Metz, O. Michel, and J.-F. Pinton, "Measurement of Lagrangian velocity in fully developed turbulence," Phys. Rev. Lett. **87**, 214501 (2001)]. The correlation structure and spectral properties of the real and modeled fields agree well under certain time dependency conditions. The correlation signature of Lagrangian accelerations is shown to reflect the persistence of the underlying streamline structure. Intermittency may influence these correlations but is not their primary cause. © *2005 American Institute of Physics*. [DOI: 10.1063/1.1852578]

I. INTRODUCTION

A. Simulation of turbulent diffusion in intermittent flows

Fully developed turbulent flows consist of motions of fluid that occupy a wide range of scales. The classical picture of such a flow is the energy cascade,[1,2] in which energy is injected into the flow by the largest scales of fluid motion whose size are of the order of the flow geometry and passed down to smaller, but equally space-filling, motions via vortex stretching and breakdown. This process is continued until the motions are small enough that viscosity becomes the leading order force and the energy is dissipated. Quantitative predictions based on this process[3] assume that the dissipative scales of the turbulence can be fully described by the kinematic viscosity of the fluid, ν, and the spatial average of the rate of energy dissipation $\langle \epsilon \rangle$. He also assumed that as long as the turbulent flow's Reynolds number is high enough the inertial range motions (i.e., the motions where energy is neither injected nor dissipated) depend only on $\langle \epsilon \rangle$. From these assumptions it can be said that for a velocity component (i.e., $i=1,2,3$) difference, $u_i(\mathbf{x}+\mathbf{r})-u_i(\mathbf{x})$, where r is in the inertial range, the following relationship holds:

$$\langle [u_i(\mathbf{x}+\mathbf{r}) - u_i(\mathbf{x})]^q \rangle \sim (r\langle \epsilon \rangle)^{\zeta_q}, \tag{1}$$

where

$$\zeta_q = \frac{q}{3} \tag{2}$$

for any component i in isotropic turbulence.

However, in recent years, experimental evidence[4,5] clearly shows that ζ_q does not scale linearly with q, suggesting that intermittency (i.e., significant spatial and temporal regions of quiescence followed by regions of highly intense activity) exists. Even in direct numerical simulations[6] (DNS) the Eulerian energy spectrum exponent p [see Eq. (13)], deviates from Kolmogorov's value of $p=5/3$, indicating intermittency.

Intermittency is not only found in the velocity structure functions, however. In studying the advection of a passive scalar,

$$\frac{\partial}{\partial t}\theta + \mathbf{u} \cdot \boldsymbol{\nabla}\, \theta = \kappa \nabla^2 \theta + f(\mathbf{x},t), \tag{3}$$

both laboratory experiments[7] and numerical simulations[8] of turbulence exhibit anomalous scaling for the structure function exponents ζ_q in

$$\langle [\theta(\mathbf{x}+\mathbf{r}) - \theta(\mathbf{x})]^q \rangle \sim r^{\zeta_q}. \tag{4}$$

In fact, eventual saturation of these exponents as q increases is observed.[9]

A naïve view of these two phenomena may expect the nonlinear scaling in Eq. (4) to follow trivially from the nonlinear scaling in Eq. (1). However, this is not so; during the 1990s, much work was presented based on the so-called Kraichnan model where velocities are modeled by

[a)]Electronic mail: david.osborne@imperial.ac.uk
[b)]Electronic mail: j.c.vassilicos@imperial.ac.uk
[c)]Electronic mail: j.haigh@ic.ac.uk

$$\langle u_i(\mathbf{x},t)u_j(\mathbf{x}',t')\rangle = 2\delta(t-t')D_{ij}(\mathbf{x}-\mathbf{x}') = 2\delta(t)r^h\left[(h+d-1)\delta_{ij} - h\frac{r_i r_j}{r^2}\right], \quad (5)$$

where $r_i = x_i - x_i'$, $r = |\mathbf{x}-\mathbf{x}'|$, d is the Euclidean dimension, and h is an exponent such that $0 < h < 2$ ($h = \frac{1}{3}$ in the case of Kolmogorov turbulence). Reference 10 and subsequent studies[11,12] investigated the relation between q-particle statistics and q-order structure functions and found that, despite the velocity field being both Gaussian and δ-correlated in time, the scalar's structure function exponents ζ_q, nevertheless, do hold the signature of intermittency.

In related work, both numerical and laboratory studies find strongly non-Gaussian behavior in the probability density functions (PDF) separation velocities.[13,14] Comprehensive reviews of all the work on structure function intermittency (be it velocity or scalar, Eulerian or Lagrangian) are available.[9]

Despite all the studies on particle-pair and multiple-particle evolution intermittency, little work has addressed the specific case of one-particle trajectories. However, recent experiments[15,16] claim to show strong evidence for one-particle Lagrangian intermittency in a von Kármán flow (see Sec. III for a description). They find this evidence in two measures: the nonlinear scaling of ξ_q in the Lagrangian structure functions and the long-time correlations of the strengths of Lagrangian accelerations, which they argue to be a key feature of the underlying intermittency.

We investigate whether a Gaussian velocity field generates one-particle Lagrangian intermittency the way it generates two-particle, and indeed, multiparticle intermittency.[17] For the velocity field we use a form of kinematic simulation and show that signatures of intermittency do not exist in the Lagrangian structure function's scaling exponent ξ_q, which shows a resolutely linear dependence on q. However, we do observe long-time correlations in the acceleration strengths. Persistence of the streamline structure in the flow would seem to be the key variable in the production of this signature rather than intermittency as defined by the nonlinear scaling of ξ_q.

In addition, a recent experiment[15] has obtained a number of Lagrangian statistical measures which provide an excellent opportunity to undertake a comparison of kinematic simulation against laboratory experiment. This comparison is presented here first, before the investigation of the intermittency.

B. Kinematic simulation

Kinematic simulation (KS) is a method for simulating Lagrangian statistics and turbulent diffusion properties that is based on a kinematically obtained Eulerian velocity field that is incompressible and consistent with Eulerian statistics up to the second order, such as the the energy spectrum $E(k)$ in wavenumber space. There is no assumption of Markovianity at any level. Instead, a persistence parameter λ controls the degree of unsteadiness of the turbulence. It is worth mentioning that when the prescribed energy spectrum has the form $E(k) \sim k^{-5/3}$ the model is in good agreement with laboratory experiments for two-particle statistics,[18] three-particle statistics,[17] and concentration variances[19] (the term "particle" that is used here is interchangeable with "fluid element"). KS is also in good agreement with DNS for two-particle statistics.[14]

The velocity of a particle at a point $\mathbf{x}$ and a time t, is constructed, in the case of homogeneous turbulence, by the summation of independent, randomly orientated, Fourier modes. These modes represent the contribution of a finite number of turbulent modes in the inertial range of the Eulerian energy spectrum. Hence kinematic simulation only models the flow field in a qualitative and highly reduced sense. What is not modeled in kinematic simulation are the phase correlations between Fourier modes, their interactions, and their dynamics. Lagrangian statistics are achieved by synthesizing physical space only along particle trajectories.

The formulation of the velocity field used in this study follows from more recent kinematic simulation studies.[19,20] The KS velocity field is kinematically prescribed to be

$$\mathbf{u}(\mathbf{x},t) = \sum_{n=0}^{N_k} \mathbf{a_n}\cos(\mathbf{k_n}\mathbf{x} + \omega_n t) + \mathbf{b_n}\sin(\mathbf{k_n}\mathbf{x} + \omega_n t), \quad (6)$$

where N_k is the total number of representative Fourier modes, $\mathbf{a_n}$ and $\mathbf{b_n}$ are the decomposition coefficients corresponding to the wavevector $\mathbf{k_n}$ and ω_n is the unsteadiness frequency.

The wavevector

$$\mathbf{k_n} = k_n\hat{\mathbf{k}}_\mathbf{n} \quad (7)$$

is randomly orientated by a random choice of $\hat{\mathbf{k}}_\mathbf{n}$. The wavenumber are distributed via

$$k_n = k_1\left(\frac{k_{N_k}}{k_1}\right)^{(n-1)/(N_k-1)}, \quad (8)$$

with n being an integer such that $1 \leqslant n \leqslant N_k$. Reference 19 found that this formulation resulted in the quickest convergence of the Lagrangian statistics.

To ensure the Fourier modes' orientations are random and the velocity field still satisfies incompressibility, the orientations of $\mathbf{a_n}$ and $\mathbf{b_n}$ are chosen independently and randomly in a plane normal to $\mathbf{k_n}$, i.e.,

$$\mathbf{a_n}\cdot\mathbf{k_n} = \mathbf{b_n}\cdot\mathbf{k_n} = 0. \quad (9)$$

Furthermore, magnitudes of $\mathbf{a_n}$ and $\mathbf{b_n}$ are chosen to conform with the prescribed energy spectrum $E(k)$, i.e.,

$$|\mathbf{a_n}|^2 = |\mathbf{b_n}|^2 = 2E(k_n)\Delta k_n, \quad (10)$$

where

$$\Delta k_n = \begin{cases} \dfrac{k_2 - k_1}{2}, & n = 1 \\ \dfrac{k_{n+1} - k_{n-1}}{2}, & n \in [2, N_k - 1] \\ \dfrac{k_{N_k} - k_{N_k - 1}}{2}, & n = N_k. \end{cases} \quad (11)$$

The Eulerian energy spectrum $E(k)$ is the main input in kinematic simulation of homogeneous isotropic turbulence (along with a coefficient of the unsteadiness frequency as we see later on in this section). The inertial range form of the energy spectrum[3] is

$$E(k) = C_K \epsilon^{2/3} k^{-5/3}, \tag{12}$$

where ϵ is the rate of dissipation of kinetic energy per unit mass and C_K is the Kolmogorov universal constant. In this study, KS only models the inertial range of the spectrum unless explicitly stated; hence k is within the surrogate inertial range, $k_1 < k < k_\eta$, where $k_\eta \equiv k_{N_k}$. We use the term "surrogate" to indicate that, in KS, the range $k_1 < k < k_\eta$ is not dynamically inertial but simply the range over which the K41 spectrum[3] is prescribed to hold.

It is also the purpose of this study to consider departures from Kolmogorov's $-5/3$ law, either as a reflection of intermittency or for the purpose of experimenting with the dependence of various Lagrangian statistics[20–22] on the scaling of $E(k)$. We therefore write the general form of the energy spectrum

$$E(k) = C_T u_{rms}^2 L (kL)^{-p}, \tag{13}$$

where $L = 2\pi/k_1$ and $p > 1$ to ensure that there is no infinite energy at the small scales when k_η is taken to infinity. The dimensionless constant $C_T = C_T(p, k_1, k_\eta)$ is such that

$$\frac{3u_{rms}^2}{2} = \int_{2\pi/L}^{2\pi/\eta} E(k)dk, \tag{14}$$

where $\eta = 2\pi/k_\eta$. The form [Eq. (13)] of the spectrum is unambiguous in KS where turbulence dynamics are absent and therefore ϵ is not directly defined. However, by using the cornerstone turbulence relation[2]

$$\epsilon = C_\epsilon \frac{u_{rms}^3}{L}, \tag{15}$$

where C_ϵ is a dimensionless constant, Eq. (13) reduces to Eq. (12) for $p = -5/3$ when $C_K C_\epsilon^{2/3} = C_T$.

Unless otherwise stated, the value of p is set to $5/3$ in this study. The value of C_ϵ does not need to be set as an input in our simulation and it should not be expected to be equal to corresponding values published in the literature as L is not the integral lengthscale.

Time dependence is introduced via the "unsteadiness frequency" ω_n, which we take to be proportional to the eddy turnover frequency of the mode n,

$$\omega_n = \lambda \sqrt{k_n^3 E(k_n)}, \tag{16}$$

where λ is the unsteadiness or "persistence" parameter which, as will be seen in later sections, can have a significant effect on one-particle two-time Lagrangian statistics.[20–22] Values of λ equal to, or very close to, zero generates a velocity field that is frozen or approximately frozen in time, i.e., a velocity field with infinite, or near-infinite, persistence in time. The other extreme of very large values of λ generates extremely unsteady velocity fields with very fast time variations and very little persistence of flow structure.

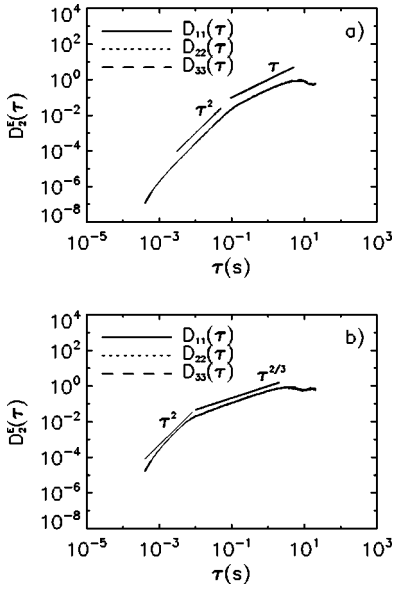

FIG. 1. Eulerian time second-order structure function, $D_2^E(\tau) = \langle [u_1(t+\tau;\mathbf{x}) - u_1(t;\mathbf{x})]^2 \rangle$, for different formulations of time dependency, (a) $\omega_n = 0.5\sqrt{k_n^3 E(k_n)}$ and (b) $\omega_n = 0.5 u_{rms} k_n$. Ballistic and the expected inertial-range scalings are observed. Due to isotropy ensures the curves turn out to be plotted on top of each other.

In Sec. II we investigate the properties of the Eulerian field simulated by kinematic simulation and show that the statistics produced are consistent with established theory. In Sec. III we use kinematic simulation to reproduce Lagrangian statistics measured in a laboratory experiment. Section IV deals with the phenomena of Lagrangian intermittency. In Sec. V we summarize the results and draw conclusions.

II. EULERIAN FIELD PROPERTIES

Although much of this study is dedicated to Lagrangian statistics it is desirable to first look at the characteristics of the model in the Eulerian frame. Tests to verify the isotropy, homogeneity, and stationarity of the turbulent flow were completed and the flow was found to satisfy

$$\langle \mathbf{u}(\mathbf{x}) \rangle = 0, \tag{17}$$

where the brackets denote an average over time so that Eq. (17) is actually found to hold at many different points $\mathbf{x}$ in the flow; it was also found that

$$\langle \mathbf{u}(t) \rangle = 0, \tag{18}$$

where the brackets denote an average over space so that Eq. (18) is found to hold at many different times t. Furthermore, it was checked that

$$\langle u_1(\mathbf{x},t)^2 \rangle = \langle u_2(\mathbf{x},t)^2 \rangle = \langle u_3(\mathbf{x},t)^2 \rangle, \tag{19}$$

where $\mathbf{u} = (u_1, u_2, u_3)$ and the averages are taken over space or over time.

The second-order one-point two-time Eulerian structure function is defined as

TABLE I. Run specification for the Eulerian field test. N_t is the number of time steps Δt or iterations $\mathbf{r}$ in each sample set. N_R is the number of KS flow field realizations and N_p is the number of sample sets per realization.

$k_1(2\pi m^{-1})$	$k_\eta(2\pi m^{-1})$	N_k	u_{rms} (m s^{-1})	λ	N_t	Δt (s)	N_R	N_p
1.0	1000.0	100	1.0	0.5	100 000	0.000 201 9	100	100

$$D_2^E(\tau) = \langle [u_i(\mathbf{x};t+\tau) - u_i(\mathbf{x};t)]^2 \rangle, \tag{20}$$

where the brackets denote an average over time. This quantity is particularly important as it is prescribed in many stochastic models whereas it is obtained here directly from the simulation; results for $i=1$ are presented in Fig. 1 (statistical homogeneity and isotropy of the field precludes the need to show results for $i=2$ and $i=3$). It was also verified that $D_2^E(\tau)$ is independent of $\mathbf{x}$. The flow parameters are all shown in Table I.

It is obvious that the moment should scale as $D_2^E(\tau) \sim \tau^2$ in the ballistic regime, i.e., for times on the order of the Kolmogorov timescale, $t_\eta = 2\pi/k_{N_k}$, or smaller. However, its scaling in the inertial range is not so obvious. Tennekes[23] proposed that the Eulerian frequency spectrum $\Phi_{11}^E(\omega)$ should scale as $\omega \sim -\frac{5}{3}$ in the inertial range, $t_\eta \ll t \ll T_E$ (where T_E is the Eulerian integral timescale), by adopting a generalization of the concept of advective spectral broadening (i.e., resulting from advection of the vorticity field by the velocity field). This is different from the Kolmogorov scaling form $\epsilon\omega^{-2}$. In other words

$$\Phi_{11}^E(\omega) \sim \omega^{-m} \tag{21}$$

for large enough ω, where $m=5/3$ as opposed to $m=2$. Since the velocity structure function can be related to the Eulerian frequency spectrum by

$$D_2^E(\tau) = 2\int_0^\infty (1 - \cos\omega\tau)\Phi_{11}^E(\omega)d\omega \tag{22}$$

we recover the relation

$$D_2^E(\tau) \sim \tau^{m-1} \tag{23}$$

for small enough τ. Hence $D_2^E(\tau) \sim \tau^{2/3}$ if $m=-5/3$ and $D_2^E(\tau) \sim \tau$ if $m=2$. Figure 1(a) suggests that $D_2^E(\tau) \sim \tau$ in the inertial range when the kinematic simulation's time dependence is controlled by Eq. (16) for both large and small values of λ. However, a different form of the time dependence, which we introduce in Sec. III C, based on an approximation of small-scale sweeping leads to $D_2^E(\tau) \sim \tau^{2/3}$ [see Fig. 1(b)].

The structure function settles to a constant value for long enough times (not obvious on the log-log plot) which is consistent with the constant term $2\langle \mathbf{u}^2 \rangle$ in

$$D_2^E(\tau) = 2\langle \mathbf{u}^2 \rangle - 2\langle \mathbf{u}(t+\tau)\mathbf{u}(t) \rangle \tag{24}$$

becoming dominant for $\tau \gg T_E$ where $\langle u(t+\tau)u(t) \rangle \approx 0$.

Now that the Eulerian field time dependence has been verified it is, perhaps, natural to look at the field's spatial structure. Figure 2 shows the two-point Eulerian velocity autocorrelation coefficients determined by

$$R_{ii}^E(\mathbf{r}) = \frac{\langle u_i(\mathbf{x}+\mathbf{r};t)u_i(\mathbf{x};t) \rangle}{\langle u_i(\mathbf{x};t)^2 \rangle}, \tag{25}$$

where there is no summation implied over the indices. The autocorrelations are taken by choosing $\mathbf{r}$ along the x axis and iterating in the Eulerian frame, obtaining $R_{11}^E(r)$ by correlating lagged values of u_1, $R_{22}^E(r)$ by correlating lagged values of u_2, and $R_{33}^E(r)$ by correlating lagged values of u_3. Averages are taken over $\mathbf{x}$ and N_R flow realizations (see Table I). The form of this result shows good agreement with theory,[24] predicting a slower decorrelation of $R_{11}^E(\mathbf{x})$ with both the $R_{22}^E(\mathbf{x})$ and $R_{33}^E(\mathbf{x})$ showing significant negative loops.

In summary we can say that a kinematically simulated Eulerian velocity field has been simulated for which it is shown that the expected scaling in the inertial range is achieved for $D_2^E(\tau)$, and that the spatial velocity correlations show good agreement with classical theory.

III. ONE-PARTICLE TWO-TIME LAGRANGIAN STATISTICS

One-particle Lagrangian statistics have been somewhat neglected when considering kinematic simulations, largely due to their satisfactory reproduction of two-particle results.[14] The exceptions[20,25] produced limited one-particle results for initial model comparison. However, recent laboratory experiments[15] have succeeded in obtaining one-particle two-time Lagrangian statistics in a fully developed turbulent flow. This gives new impetus to numerical models producing one-particle statistics, and provides an excellent opportunity for a first ever comparison of KS one-particle two-time predictions using experimental data.

A. The laboratory flow

The turbulent flow of the experiment[15] is created between two counterrotating disks forming a so-called swirling

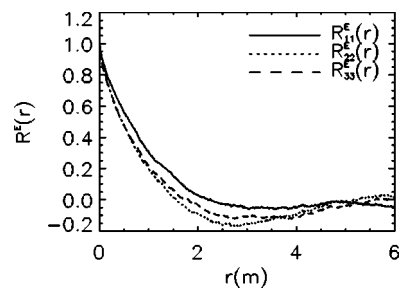

FIG. 2. Eulerian two-point velocity correlations, $R_{ii}^E(\mathbf{r}) = \langle u_i(\mathbf{x}+\mathbf{r};t)u_i(\mathbf{x};t) \rangle / \langle u_i(\mathbf{x};t)^2 \rangle$. The longitudinal curve shows a slower decorrelation than the transverse curves, the latter exhibiting negative loops. Averages are taken over flow realizations.

TABLE II. Run specification for the kinematic simulation flow attempting to reproduce the experiments of Refs. 15 and 16. Here N_t is the number of time steps per Lagrangian fluid element trajectory. N_R is the number of KS flow realizations and N_p is the number of fluid element trajectories per realization.

$k_1(2\pi m^{-1})$	$k_\eta(2\pi m^{-1})$	N_k	u_{rms} (m s^{-1})	N_t	Δt (s)	N_R	N_p
62.83	71 400.0	100	0.98	33 200	3.0126$E-6$	100	100

von Kármán flow.[26] In this way, it is claimed, large experimental Reynolds numbers can be obtained ($\mathrm{Re}_\lambda = 740$ in the case used here). Neutrally buoyant polystyrene spherical particles seed the sonified fluid and ultrasonic acoustical techniques[27] are used to track their trajectory.

The experiment[15] claims to reproduce a good approximation of isotropic and homogeneous turbulence in a section in the middle of a cylinder that constrains the flow between the counterrotating disks. This section has a 10 cm extent in the axial direction and extends almost the whole diameter of the cylinder which is itself 9.5 cm wide. Therefore, it was decided that k_1 should be representative of these large scale motions (see Table II).

Although, experimentally, this type of swirling flow achieves between one and a half and two wavenumber decades of $-5/3$ scaling in the inertial subrange,[26,28] the experiment claims to achieve a high Reynolds number compared to other laboratory turbulent flows, high enough for the results to be close to their high-Reynolds-number asymptotic analogs. This is why we have spanned approximately three decades of wavenumbers in the kinematic simulation. This range is consistent with us choosing both $L \approx 10$ cm and $\eta = 88$ μm, a tenth of the experiment's[15] Taylor microscale. Although a Kolmogorov lengthscale of 60 μm can be determined using the microscale relationships, $\eta = (\nu^3/\epsilon)^{1/4}$, due to the temporally unstable nature of the power being inputted by the rotating disks[29] it was decided not to base η on the stated dissipation rate ($\epsilon = 25$ W/kg). A summary of all the KS parameters is presented in Table II.

B. Lagrangian velocity correlations

The experimental study[15] calculates the Lagrangian velocity component autocorrelations,

$$R_{ii}^L(\tau) = \frac{\langle v_i(t+\tau) v_i(t) \rangle}{\langle v_i(t)^2 \rangle}, \tag{26}$$

where $v_i(t) = u_i[\mathbf{x}(t), t]$, no summation is implied over indices and the averages are taken over time t and N_R flow realizations; there are N_p trajectories per realization (see Table II). $R_{11}^L(\tau)$ is the only component measured, presumably due to limitations of the experimental setup.

Their experiment is run for ≈ 0.1 s (or five Lagrangian integral timescales) and it is observed from our corresponding calculation, Fig. 3, that kinematic simulation, using $\lambda = 0.1$, is in excellent quantitative agreement with (we also present $i = 2,3$ to further enhance the idea of an isotropic model), with the velocity completely decorrelating within ≈ 0.08 s. The value of λ was chosen to obtain the best quantitative agreement, however, it is important to point out that the qualitative nature of the Lagrangian statistics presented in this section (i.e., the exponential decay of the Lagrangian autocorrelations and the scaling of the Lagrangian structure functions and spectra) are invariant for $\lambda < 1.0$.[22] Of course the Eulerian field is insensitive to any change in the time dependency of the simulation.

A more useful value that can be extracted from this result is the integral, or characteristic, timescale of the flow, which is usually determined by

$$T_{L_i} = \int_0^\infty R_{ii}^L(\tau) d\tau, \tag{27}$$

where $T_{L_1} = T_{L_2} = T_{L_3} = T_L$ for isotropic turbulence. Mordant *et al.*[15] choose to fit an exponential decay curve of the form $R_{11}^L(\tau) \sim e^{-\pi/T_L}$ to the data. We employ the same method (Fig. 4). Mordant *et al.*[15] obtain the exponential function

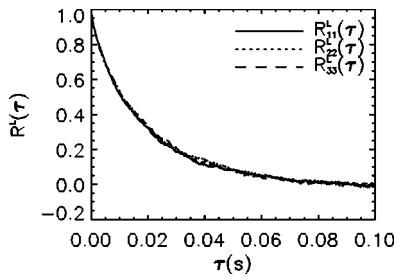

FIG. 3. Lagrangian velocity correlations, $R_{ii}^L(\tau) = \langle v_i(t+\tau) v_i(t) \rangle / \langle v_i(t)^2 \rangle$. Averages are taken over Lagrangian fluid element trajectories. All curves show excellent agreement with experiment [see Fig. 1(a) of the work by Mordant *et al.*].

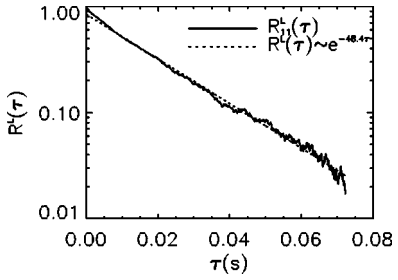

FIG. 4. Exponential function fit, $R_{11}^L(\tau) \sim e^{-\pi/T_L}$, of the Lagrangian velocity correlation, $R_{ii}^L(\tau) = \langle v_i(t+\tau) v_i(t) \rangle / \langle v_i(t)^2 \rangle$. Data after ≈ 0.07 s are discarded so that noisy data do not bias the fitting. The integral timescale was calculated as $T_L = 20.7$ ms.

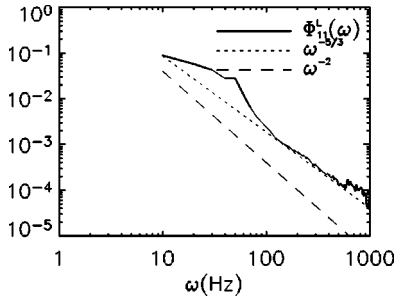

FIG. 5. Lagrangian velocity power spectrum $\Phi^L_{11}(\omega)$ averaged with a simple 10 Hz sliding window. The persistence parameter $\lambda=0.1$. Despite being calculated in a Lagrangian frame, the spectrum exhibits Eulerian scaling ($\omega^{-5/3}$) rather than Kolmogorov scaling (ω^{-2}).

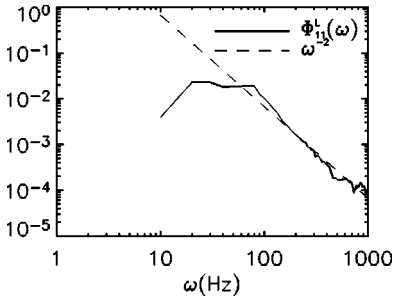

FIG. 7. Lagrangian velocity power spectrum $\Phi^L_{11}(\omega)$ averaged with a simple 10 Hz sliding window. The persistence parameter $\lambda=5.0$. Some evidence on Kolmogorov scaling is observed (ω^{-2}).

$$R^L_{11}(\tau) = 1.03e^{-45.7\tau}, \tag{28}$$

which yields an integral timescale of 21 ms. The kinematic simulation data produces the exponential function

$$R^L_{11}(\tau) = 0.84e^{-48.3\tau}. \tag{29}$$

The value of $R^L_{11}(\tau)$ shows some variation from both the exponential form and the experimental data at small times, however, note that the KS result yields $T_L=20.7$ ms, which is in good agreement with the experiment. T_L can also be estimated from Corrsin's relation $T_L \sim \mathcal{L}/u_{rms}$, where $\mathcal{L}$ is the integral lengthscale, which, in the case of isotropic homogeneous turbulence can be calculated using the formula[24]

$$\mathcal{L} = \frac{3\pi}{4}\frac{\int_0^\infty k^{-1}E(k)dk}{\int_0^\infty E(k)dk}. \tag{30}$$

This procedure yields a value of $T_L=15.1$ ms which is consistent with $T_L=21$ ms considering that the scaling constant in $T_L \sim \mathcal{L}/u_{rms}$ is close to 1.

C. The Lagrangian and Eulerian velocity power spectra

The next analysis that Mordant *et al.*[15] undertake is to construct the Lagrangian velocity power spectrum using the real part of the Fourier transform,

$$\Phi^L_{11}(\omega) = u^2_{rms}\int_0^\infty R^L_{11}(\tau)e^{-i\omega\tau}d\tau. \tag{31}$$

They claim that a scaling of $\Phi^L_{11}(\omega)\sim\omega^{-2}$ is achieved, as predicted by theory.[30,23] In fact, Mordant *et al.*[15] compare their measured spectrum to the Lorentzian function,

$$\Phi^{Fit}_L(\omega) = \frac{u^2_{rms}T_L}{1+(T_L\omega)^2}. \tag{32}$$

Presumably this is to try and incorporate at least some of the effect that the large-scale energy-containing motions have on the spectral shape. Using a simple sliding 10 Hz nonoverlapping averaging window, the spectrum produced by the KS model for $\lambda=0.1$ is depicted in Fig. 5. It is clear that the agreement with $\Phi_L(\omega)\sim\omega^{-2}$ is not good. In fact the Lagrangian power spectrum produced by the kinematic simulation scales like the *Eulerian* spectrum.[23] According to Ref. 22, this is attributable to the low persistence parameter λ used in this run. A kinematic simulation such as the one used here does not incorporate sweeping of the small-scale eddies by the large ones, and it should, perhaps, not be expected, in general, that KS should reproduce either $\Phi_L(\omega)\sim\omega^{-2}$ or $\Phi_E(\omega)\sim\omega^{-5/3}$ (the advective spectral broadening of Ref. 23 referred to in Sec. II). However, we do observe $\Phi_E(\omega)\sim\omega^{-5/3}$ for both large and small values of lambda (see Fig. 6) and in the case of large λ, e.g., $\lambda=5$ as in Fig. 7, $\Phi_L(\omega)\sim\omega^{-2}$ is also observed as previously reported.[22]

However, returning to the Lagrangian velocity autocorrelation using this high value of λ we find that all quantitative, and, indeed qualitative, agreement with the laboratory

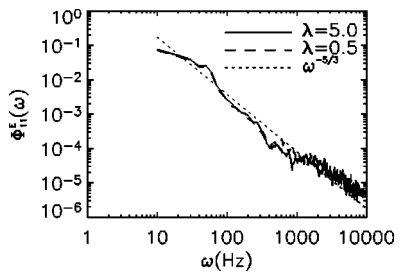

FIG. 6. Eulerian velocity power spectrum $\Phi^E_{11}(\omega)$ averaged with a simple 10 Hz sliding window. The spectrum is insensitive to the time dependency of the kinematic simulation velocity field. Correct scaling as predicted by Ref. 23 is observed ($\omega^{-5/3}$).

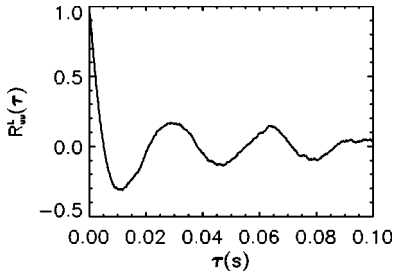

FIG. 8. Lagrangian velocity correlations, $R^L_{11}(\tau)=\langle v_1(t+\tau)v_1(t)\rangle/\langle v_1(t)^2\rangle$. Averages are taken over Lagrangian fluid element trajectories. The persistence parameter $\lambda=5.0$. All quantitative and qualitative agreement seen in Fig. 3 is lost.

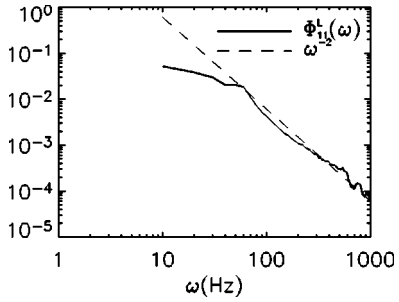

FIG. 9. Lagrangian velocity power spectrum $\Phi^L_{11}(\omega)$ averaged with a simple 10 Hz sliding window. Here, $\omega_n = \lambda u_{rms} k_n$. Kolmogorov scaling ($\omega^{-2}$) is recovered.

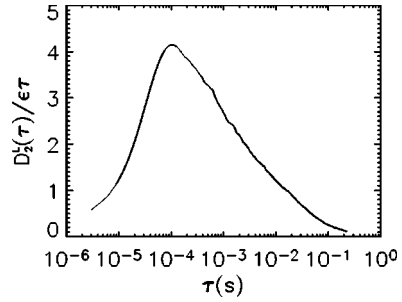

FIG. 11. The Lagrangian second-order structure function, $D^L_2(\tau) = \langle [v_1(t+\tau) - v_1(t)]^2 \rangle$, compensated with time, $D^L_2(\tau)/\epsilon\tau$. The persistence parameter $\lambda = 0.1$. Averages are taken over fluid element trajectories. No scaling $D^L_2(\tau) \sim \tau$ is observed; we have checked that this structure function instead scales as $D^L_2(\tau) \sim \tau^{2/3}$.

results obtained with $\lambda = 0.1$ is lost (see Fig. 8). And here is the crux of the problem of the persistence parameter effect. The role of the unsteadiness frequency is not limited to reproducing the sweeping effect on the frequency spectra without actual sweeping; it also, of course, largely determines the integral timescales of the flow and it is found that T_L decreases as λ increases.

A possible solution to the problem is to replace our ω_n model by an alternate formulation of the unsteadiness frequency,

$$\omega_n = \lambda u_{rms} k_n. \tag{33}$$

Here, we simplify the sweeping mechanism by sweeping all scales with one average velocity u_{rms}. Clearly the assumption of an average neglects both the time dependency of the large-scale sweeping velocities and their direction. However, on average, this formulation, although incomplete and inaccurate, may go some way in representing the sweeping of the small-scales eddies by the large energy-containing ones.

Using this formulation we calculate again the Lagrangian velocity power spectrum [Eq. (31)] and the Lagrangian velocity autocorrelation [Eq. (26)] using a low persistence parameter ($\lambda = 0.1$). From Fig. 9 we can see the sweeping on $\Phi_L(\omega)$ and it can be argued that the scaling, $\Phi_L(\omega) \sim \omega^{-2}$, is, in fact, even better than in Fig. 7. The autocorrelation curve (Fig. 10) still exhibits a significant negative loop, compromising the accurate determination of the Lagrangian integral timescale T_L. However, it certainly is an improvement over the rapidly oscillating curve in Fig. 8 and if this model was to be used in conjunction with a convective range model that explicitly simulates the large scales (for example, large-eddy simulation (LES)-KS hybrid approach[19]), then it is entirely conceivable that the single negative loop would be eradicated.

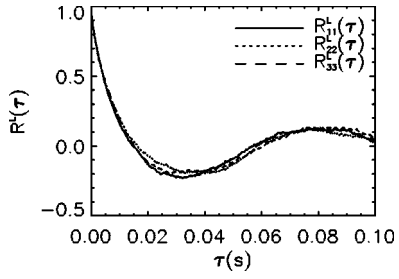

FIG. 10. Lagrangian velocity correlations, $R^L_1(\tau) = \langle u_1(t+\tau)u_1(t) \rangle / \langle u_1(t)^2 \rangle$. Averages are taken over fluid element trajectories. The persistence parameter $\lambda = 0.1$. A negative loop is still observed although not as dominant as the loops in Fig. 8.

To summarize, we have used the experimental results of Mordant *et al.*[15] to compare the Lagrangian statistics that can be extracted from a time-varying, kinematically simulated, Eulerian velocity field. We find excellent quantitative agreement when comparing the Lagrangian velocity autocorrelations for a weakly time-dependent KS field. This weak time dependency leads to anomalous, that is Eulerian, scaling in the Lagrangian velocity power spectrum. This was rectified with a strongly time-dependent velocity field but at the expense of any agreement in the correlation structure of the flow. A compromise was made with a different formulation of the time-dependent terms in the velocity field which gave excellent agreement with experimental measurement of the Lagrangian velocity power spectrum and an acceptable form of the autocorrelogram.

IV. LAGRANGIAN INTERMITTENCY

A. Lagrangian structure functions

We first look at the second-order Lagrangian structure function {it should be noted that for the remainder of the paper we revert to the original formulation of the unsteadiness frequency [Eq. (16)]}, which, in view of isotropy, can be defined as

$$D^L_2(\tau) = \langle [v_1(t+\tau) - v_1(t)]^2 \rangle, \tag{34}$$

where the average is taken over time t and N_R trajectories. We plot it in a compensated way (as do Mordant *et al.*[15]) in Fig. 11 that will expose any inertial range scaling, i.e.,

$$D^L_2(\tau) = \langle [v_1(t+\tau) - v_1(t)]^2 \rangle \sim \epsilon\tau, \tag{35}$$

which, for a valid range of frequencies ω, corresponds to $\Phi^L_{11}(\omega) \sim \epsilon\omega^{-2}$ via the relation

$$D^L_2(\tau) = 2\int_0^\infty (1 - \cos\omega\tau)\Phi^L_{11}(\omega)d\omega. \tag{36}$$

As should be expected from the absence of $\Phi^L_{11}(\omega) \sim \omega^{-2}$ scaling for small λ with $\omega_n = \lambda\sqrt{k_n^3 E(k_n)}$, the scaling

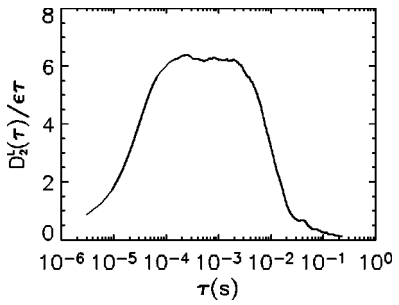

FIG. 12. The Lagrangian second-order structure function, $D_2^L(\tau)=\langle[v_1(t+\tau)-v_1(t)]^2\rangle$, compensated with time, $D_2^L(\tau)/\epsilon\tau$. The persistence parameter $\lambda=5.0$. Averages are taken over N_p Lagrangian fluid element trajectories for N_R flow realizations. A significant range of the scaling $D_2^L(\tau)\sim\tau$ is observed.

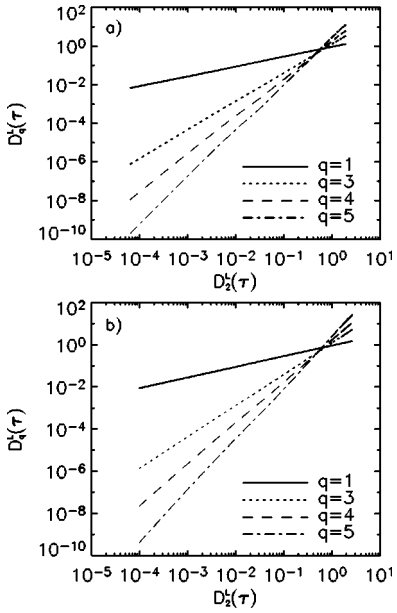

FIG. 13. Extended self-similarity ansatz, $D_q^L(\tau)\sim D_2^L(\tau)^{\xi_q/\xi_2}$, for several orders of the structure functions, $D_q^L(\tau)=\langle[v_l(t+\tau)-v_l(t)]^q\rangle$. Each figure represents a simulation run with a different value of persistence parameter (a) $\lambda=0.1$ and (b) $\lambda=5.0$. The same scaling is observed over the same wide range for both high and low values of the persistence parameter.

plateau is not observed for $\lambda=0.1$. Initially this may be seen as a good thing since none is observed in the experiment either (although the authors claim to achieve such a scaling regime, the range is too small to unambiguously distinguish a plateau from a peak). However, whereas in the latter study the problem comes primarily from the relatively low Reynolds number, in the kinematic simulation this is not the problem since $L/\eta\sim10^3$. So although the agreement is good it is probably coincidental and we are seeing a Lagrangian structure function that is, in fact, scaling as $\tau^{2/3}$, corresponding to the $\omega^{-5/3}$ of the Eulerian spectrum and of the Lagrangian spectrum for $\omega_n=\lambda\sqrt{k_n^3E(k_n)}$ with low values of λ (see Sec. III C). If, however, the unsteadiness parameter is again increased to $\lambda=5.0$ then the expected plateau is observed (Fig. 12). What is also encouraging is that the value for C_0 in $D_2^L(\tau)=C_0\epsilon\tau$ is consistent with both the experimentally derived value[31] ($C_0=4\pm2$) and the values used in stochastic models for turbulent dispersion[32] ($C_0=5\pm2$). We have reverted to using Eq. (16) to determine the unsteadiness of the flow but we find a comparable value for C_0 when using Eq. (33), as might be expected from the similar data ranges seen in Figs. 7 and 9.

Intermittency is often studied by examining the behavior of the q-order structure function

$$D_q^L(\tau)=\langle[v_l(t+\tau)-v_l(t)]^q\rangle, \tag{37}$$

where averages are taken in the same way as Eq. (34). In order to compensate for their lack of a well-defined inertial subrange, Mordant *et al.*[15] extrapolate the extended self-similarity approach[33] for two-particle Lagrangian statistics to one-particle Lagrangian statistics. In this approach, structure functions $D_q^L(\tau)$ are plotted as a function of a reference moment, say $D_2^L(\tau)$, and power law scalings are sought, i.e.,

$$D_q^L(\tau)\sim D_2^L(\tau)^{\xi_q/\xi_2}, \tag{38}$$

where ξ_q is the time scaling exponent of the structure function of order q. In the kinematic simulation results shown in Fig. 13, it is clear that such scalings do exist over a very wide range, extending over at least four decades. These scalings and their ranges appear to be independent of λ.

In the absence of inertial range intermittency in one-particle two-time Lagrangian homogeneous, isotropic turbulence, we should expect $\xi_q/\xi_2=q/2$. However, the findings of the experiment are at variance with this prediction, which suggests that their flow is intermittent. The deviation is most pronounced for the higher order statistics where the rare, strong events become detectable. In Fig. 14 we compare the values of ξ_q/ξ_2 for both the high and low persistence parameter simulations and the experiment. The deviation from non-intermittent values is clear in the experiment, whereas the values for the kinematic simulations are closely in agreement with the prediction $\xi_q=(q/2)\xi_2$, valid in the absence of inertial-range intermittency.

As noted in previous studies,[22] kinematic simulations lead to $\xi_2=p-1$ for $\lambda<1$ and $\xi_2=2(p-1)/(3-p)$ for $\lambda\gg1$, where p is the scaling exponent of the energy spectrum [see Eq. (13)]. It follows, using $\xi_q=(q/2)\xi_2$, that we should have

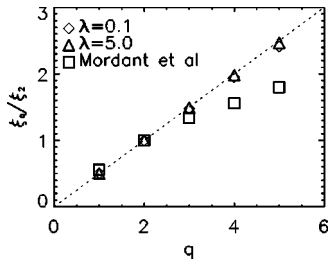

FIG. 14. Relative scaling exponents ξ_q/ξ_2 obtained by the extended self-similarity approach. In the absence of intermittency in the homogeneous isotropic velocity field the kinematic simulations scale linearly according to $\xi_q/\xi_2=q/2$ regardless of the value of λ. The exponents determined from the experiment of Ref. 15 clearly show nonlinear scaling, suggesting their flow is intermittent.

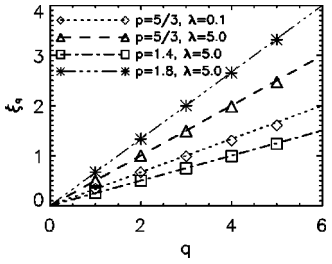

FIG. 15. Extended self-similarity scaling exponents ξ_q for $p=1.4$, $-5/3$, and 1.8. The persistence parameter is $\lambda=5.0$ for all simulations except when $p=-5/3$, in which case we use both high and low values of λ. It is clear that ξ_q can be readily changed by adopting different values of both λ and p.

$$\xi_q = \begin{cases} \dfrac{q}{2}(p-1) & \text{for } \lambda < 1.0 \\ \dfrac{q(p-1)}{3-p} & \text{for } \lambda \gg 1.0, \end{cases} \tag{39}$$

and this is indeed what we observe in Fig. 15. Eulerian intermittency of turbulent flows might well lead to a deviation of p away from the value $\frac{5}{3}$, but changes in the value of p in a turbulent-like flow without Eulerian intermittency, such as KS, do not lead to Lagrangian inertial range intermittency: ξ_q remaining proportional to q, only the constant of proportionality changes.

The absence of inertial range intermittency in one-particle Lagrangian velocity statistics obtained by KS is further revealed if we examine the PDFs of the velocity increment

$$\Delta_\tau v_1 = v_1(t+\tau) - v_1(t). \tag{40}$$

Plotting their flatness factors, $K(\tau)=\langle(\Delta_\tau v_1)^4\rangle/\langle(\Delta_\tau v_1)^2\rangle^2-3$ in Fig. 16 for high and low time dependency, we find that they remain resolutely Gaussian for all times, unlike the laboratory results which exhibit highly non-Gaussian statistics.

B. One-particle acceleration correlations in kinematically simulated, Gaussian velocity fields

A second experiment using almost identical flow parameters[16] and experimental setup investigates one-particle acceleration correlations. They define a velocity increment over a time lag τ as the total contribution of a number of velocity increments over a smaller time interval τ_1

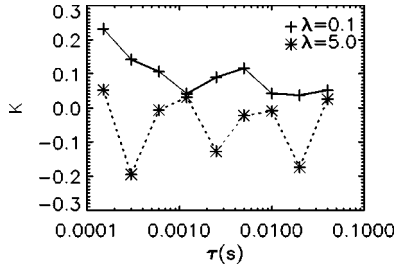

FIG. 16. Flatness factors for the PDFs of $\Delta_\tau v_1$ where $\tau=0.15$, 0.3, 0.6, 1.2, 2.5, 5.0, 10.0, 20.0, and 40.0 ms. The KS-obtained PDFs fail to show any significant flatness values at any times, regardless of the value of λ.

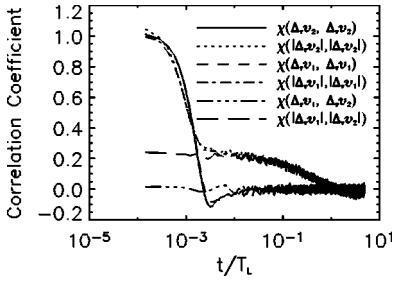

FIG. 17. Correlation coefficients, $\chi(f,g)(\Delta t)=(\langle[f(t+\Delta t)-\langle f\rangle][g\langle t\rangle-\langle g\rangle]\rangle)/\sigma_f\sigma_g$, for various velocity increments [identities can be found in Eq. (43)]. Persistence parameter $\lambda=0.1$. It is evident that the acceleration components remain correlated over long times.

$$\Delta_\tau v_1(t) = v_i(t+\tau) - v_i(t) = \sum_{n=1}^{\tau/\tau_1} \Delta_{\tau_1} v_i(t+n\tau_1). \tag{41}$$

This definition allows them to study the dependence of the elementary steps τ_1 on each other. To do this they define several correlation relationships that have the following general form:

$$\chi(f,g)(\Delta t) = \frac{\langle[f(t+\Delta t)-\langle f\rangle][g(t)-\langle g\rangle]\rangle}{\sigma_f\sigma_g}, \tag{42}$$

where σ_f and σ_g are the rms values of f and g, respectively, and all averages are calculated over time t and many particle trajectories. Many different forms of f and g were tried, for example,

$$\chi(f,g) = \begin{cases} \chi(\Delta_\tau v_2, \Delta_\tau v_2) \\ \chi(|\Delta_\tau v_2|, |\Delta_\tau v_2|) \\ \chi(\Delta_\tau v_1, \Delta_\tau v_1) \\ \chi(|\Delta_\tau v_1|, |\Delta_\tau v_1|) \\ \chi(\Delta_\tau v_1, \Delta_\tau v_2) \\ \chi(|\Delta_\tau v_1|, |\Delta_\tau v_2|). \end{cases} \tag{43}$$

Using these functions, the autocorrelations of both the signed and absolute values of $i=1$, 2 velocity increments can be determined, as well as the corresponding cross-correlations. The results produced by kinematic simulation with a persistence parameter of $\lambda=0.1$ are shown in Fig. 17. Comparing with the curves of the experiment,[16] we find excellent qualitative agreement. The signed values of the increment autocorrelations decorrelate extremely quickly, within about one Kolmogorov timescale (in Fig. 17 $\tau_\eta \approx 0.01 T_L$), with the cross-correlations confirming that the two signed velocity components are independent. This is consistent with the reasoning behind treating one-particle Lagrangian turbulence as a Markovian process where the accelerations are independent (accelerations and velocity increments are equivalent in the limit $\tau_1 \to 0$). This is the premise of stochastic models that use Langevin-type equations as their base.[34,35] However, when Mordant *et al.*[16] look at the unsigned, or absolute, values of both the autocorrelations and cross-correlations, they find significant correlations for all three measures persisting for very long times up to the integral timescale determined in Sec. III B. Mordant *et al.*[16] take this to be an indication of the intermittency of their flow.

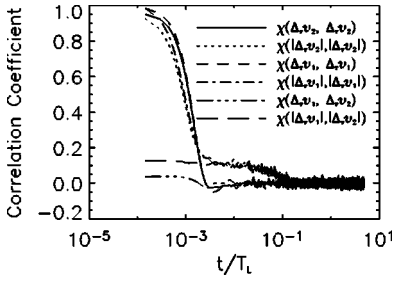

FIG. 18. Correlation coefficients, $\chi(f,g)(\Delta t)=(\langle[f(t+\Delta t)-\langle f\rangle][g(t)-\langle g\rangle]\rangle)/\sigma_f\sigma_g$, for various velocity increments [identities can be found in Eq. (43)]. Persistence parameter $\lambda=5.0$. It is clear that the increased time dependency further lowers the strength of the correlations and significantly shortens the period over which the increments are correlated.

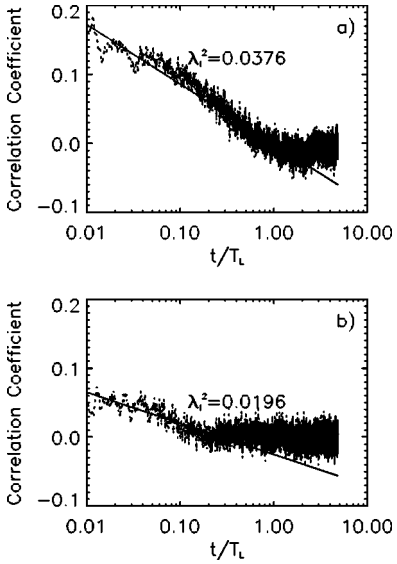

FIG. 19. Correlation coefficients, $\chi(f,g)(\Delta t)=(\langle[f(t+\Delta t)-\langle f\rangle][g(t)-\langle g\rangle]\rangle)/\sigma_f\sigma_g$ for the velocity increment $\chi(\ln|\Delta_\tau v_1|,\ln|\Delta_\tau v_1|)$. Persistence parameter (a) $\lambda=0.1$ and (b) $\lambda=5.0$. A scaling region is well defined and the "intermittency parameter" λ_I^2 decreases with increasing persistence parameter λ.

Looking at Fig. 17 it is clear that in KS we also find very long-time correlations for these velocity increments, although the strength of the correlations are significantly lower than those of Mordant *et al.*[16] (around half the laboratory experiment's strength, in fact). In Sec. IV A we present convincing results that show that kinematic simulation does not exhibit one-particle Lagrangian intermittency, and that KS has no Eulerian intermittency on account of its Gaussianity, this discovery may be, at first, surprising. Hence, the key feature underpinning the long-time correlations in Fig. 17 is not the inertial-range intermittency. One way to understand the correlations is in terms of persistent vortices. The acceleration vectors of fluid elements circling around vortices can be expected to decorrelate within a vortex turnover time, but if these vortices are persistent (in the sense of being coherent and long lived) then the acceleration strengths of the fluid element can be expected to be correlated for much longer (as observed in Fig. 17). With the great majority of the vortices being of size of the order of the Kolmogorov microscale,[21] it is expected that the Kolmogorov timescale τ_η will be the dominant decorrelation time for the acceleration vectors and this is indeed observed in Fig. 17. Such regions of high vorticity, as well as other high strain and streaming regions, are known to exist in KS.[25,20] These high vorticity regions may not have the same shape or spatial distribution as coherent vortices in real turbulence but their presence may be enough to provide the vortical regions responsible for the acceleration correlations, even though the flow is statistically Gaussian with no intermittency. The inertial-range intermittency may act to accentuate these correlations but does not seem to be the cause of their underlying signature.

To check our view that it is the persistence of the vortical streamlines that is key in producing these long-time acceleration correlations we have increased the persistence parameter to $\lambda=5.0$ (see Fig. 18). The result is that the intensity of the long-time correlation in Fig. 17 is diminished when the turbulence is made less persistent in time (i.e., increasing λ). Following the example of Mordant *et al.*[15] we take the correlation in time of the increments $\chi(\ln|\Delta_\tau v_1|,\ln|\Delta_\tau v_1|)$ and find the slope of the scaling region, the value of which they call the intermittency parameter λ_I^2 (λ_I^2 should not be confused with, or thought to be related to, the persistence parameter λ). Looking at Fig. 19 it is clear that λ_I^2 is well defined and decreases with increasing values of persistence parameter λ. For $\lambda=0.1$ the value is approximately one-third of the value predicted in the experiment,[15] $\lambda_I^2=0.0115\pm0.01$. This result supports the view that it is flow persistence and not intermittency that is primarily responsible for the long-time acceleration correlations and for the scaling of $\chi\sim\ln(t/T_L)$.

V. SUMMARY AND CONCLUSIONS

A KS model of Lagrangian dispersion has been described and Lagrangian data from laboratory experiments[15] have been used to compare with Lagrangian statistics extracted from the model. The Eulerian field that the model is based on has also been compared with classical theory; the Eulerian structure function, $D_2^E(\tau)=\langle[u_i(t+\tau;\mathbf{x})-u_i(t;\mathbf{x})]^2\rangle$, shows consistent inertial-range scaling in accordance with the formulation of unsteadiness frequency used and the Eulerian velocity autocorrelogram, $R_{ii}^E(r)=\langle u_i(\mathbf{x}+\mathbf{r};t)u_i(\mathbf{x};t)\rangle/\langle u_i(\mathbf{x};t)^2\rangle$, exhibits properties expected from Ref. 24.

Using flow parameters determined from the laboratory experiment, the Lagrangian velocity autocorrelogram, $R_{11}^L(\tau)=\langle v_1(t+\tau)v_1(t)\rangle/\langle u_1(t)^2\rangle$ shows remarkable agreement with experiment when using a small value of the persistence parameter ($\lambda=0.1$). This agreement results in the simulated and measured values of the Lagrangian integral timescale being within 2%. However, when the Lagrangian velocity power spectrum $\Phi_{11}^L(\omega)$ is plotted it is observed that $\Phi_{11}^L(\omega)\sim\omega^{-5/3}$ instead of the expected Kolmogorov scaling ω^{-2}. We attribute this effect to the lack of sweeping of smaller scales by larger ones. This effect disappears when the persistence parameter is increased to a value much greater than 1 ($\lambda=5.0$), in which case $\Phi_{11}^L(\omega)\sim\omega^{-2}$. However, large values of λ spoil the agreement seen in the Lagrangian velocity correlations. A partial compromise is reached by refor-

mulating the time dependency of the field in a way that partially takes into account large scale sweeping. From this reformulation, excellent agreement with ω^{-2} results for the velocity power spectrum and the autocorrelation curve, while not fully conforming to the expected $R^L(\tau) \sim e^{-\tau}$ form, is nevertheless a considerable improvement on the previous results obtained for large values of λ. The universal Lagrangian constant C_0, defined by $D_2^L(\tau) = C_0 \epsilon \tau$ in the inertial range, is an output of the model and the value obtained is consistent with experimentally derived values. Further improvement might be achieved by a direct calculation of the large scales in a LES-KS approach.[19]

Structure functions of order q, $D_q^L(\tau)$, plotted against $D_2^L(\tau)$ reveal a wide range of scaling for all values of q, regardless of the level of time dependency given to the flow. To evaluate the level of intermittency, their scaling exponents ξ_q have been plotted for both the simulated and the laboratory flows. The exponents derived from KS give the Kolmogorov relation for homogeneous isotropic turbulence, $\xi_q = (q/2)\xi_2$, whereas the values measured from the experiment show considerable deviation, indicating intermittency. The lack of one-particle, Eulerian intermittency in KS is confirmed by the fact that all PDFS of the velocity increment, $\Delta_\tau v_1 = v_1(t+\tau) - v_1(t)$, are strongly Gaussian for all times τ. The scaling exponents ξ_q are functions of both the persistence parameter λ and of the Eulerian input spectrum exponent p.

While signed values of the components of the acceleration vector decorrelate over times of order τ_η in KS, absolute values remain correlated for times of order T_L. It is also found that the intermittency parameter λ_I^2, introduced by Mordant *et al.*[16] remains finite for all values of persistence parameter λ. These findings were also observed in the laboratory flow albeit with higher correlation values, and was attributed to the intermittency of active turbulent regions.[16] Our results suggest that the cause of these acceleration correlation signatures is the persistence of vortical regions in the turbulence rather than intermittency. Intermittency may, however, have the effect of accentuating these signatures.

ACKNOWLEDGMENTS

D.R.O. was supported by a postgraduate studentship from the UK Natural Environment Research Council and J.C.V. acknowledges support from the Royal Society of London and the Hong Kong Research Council Grant RGC/HKUST601203.

[1] U. Frisch, *Turbulence* (Cambridge University Press, Cambridge, 1995).
[2] S. B. Pope, *Turbulent Flows* (Cambridge University Press, Cambridge, 2000).
[3] A. N. Kolmogorov, "The local structure of turbulence in incompressible viscous fluid for very large Reynolds numbers," Dokl. Akad. Nauk SSSR **30**, 301 (1941).
[4] J. Maurer, P. Tabeling, and G. Zocchi, "Statistics of turbulence between two counter-rotating disks in low temperature helium gas," Europhys. Lett. **26**, 31 (1994).
[5] A. Staicu and W. van de Water, "Small scale velocity jumps in shear turbulence," Phys. Rev. Lett. **90**, 094501 (2003).
[6] Y. Kaneda, T. Ishihara, M. Yokokawa, K. Itakura, and A. Uno, "Energy dissipation rate and energy spectrum in high resolution direct numerical simulations of turbulence in a periodic box," Phys. Fluids **15**, L21 (2003).
[7] R. A. Antonia, E. J. Hopfinger, Y. Gagne, and F. Anselmet, "Temperature structure functions in turbulent shear flows," Phys. Rev. A **30**, 2704 (1984).
[8] S. Chen and N. Cao, "Anomalous scaling and structure instability in three-dimensional passive scalar turbulence," Phys. Rev. Lett. **78**, 3459 (1997).
[9] G. Falkovich, K. Gawędzki, and M. Vergassola, "Particles and fields in fluid turbulence," Rev. Mod. Phys. **73**, 913 (2001).
[10] R. H. Kraichnan, "Anomalous scaling of a randomly advected passive scalar," Phys. Rev. Lett. **72**, 1016 (1994).
[11] K. Gawędzki and A. Kupianen, "Anomalous scaling of a passive scalar," Phys. Rev. Lett. **75**, 3834 (1995).
[12] M. Chertkov and G. Falkovich, "Anomalous scaling exponents of a white-advected passive scalar," Phys. Rev. Lett. **76**, 2706 (1996).
[13] M.-C. Jullien, J. Paret, and P. Tabeling, "Richardson's pair dispersion in two-dimensional turbulence," Phys. Rev. Lett. **82**, 2872 (1999).
[14] N. A. Malik and J. C. Vassilicos, "A Lagrangian model for turbulent dispersion with turbulent-like flow structure: comparison with direct numerical simulation for two-particle statistics," Phys. Fluids **11**, 1572 (1999).
[15] N. Mordant, P. Metz, O. Michel, and J.-F. Pinton, "Measurement of Lagrangian velocity in fully developed turbulence," Phys. Rev. Lett. **87**, 214501 (2001).
[16] N. Mordant, J. Delour, E. Léveque, A. Arnéodo, and J.-F. Pinton, "Long time correlations in Lagrangian dynamics: a key to intermittency in turbulence," Phys. Rev. Lett. **89**, 254502 (2002).
[17] M. A. I. Khan, A. Pumir, and J. C. Vassilicos, "Kinematic simulation of turbulent dispersion of triangles," Phys. Rev. E **68**, 026313 (2003).
[18] F. Nicolleau and G. Yu, "Two-particle diffusion and the locality assumption," Phys. Fluids **16**, 2309 (2004).
[19] P. Flohr and J. C. Vassilicos, "A scalar subgrid model with flow structure for large-eddy simulations of scalar variances," J. Fluid Mech. **407**, 315 (2000).
[20] J. C. Fung and J. C. Vassilicos, "Two-particle dispersion in turbulent-like flows," Phys. Rev. E **57**, 1677 (1998).
[21] J. Davila and J. C. Vassilicos, "Richardson's pair diffusion and the stagnation point structure of turbulence," Phys. Rev. Lett. **91**, 144501 (2003).
[22] M. A. I. Khan and J. C. Vassilicos, "A new Eulerian-Lagrangian length-scale in turbulent flows," Phys. Fluids **16**, 216 (2004).
[23] H. Tennekes, "Eulerian and Lagrangian time microscales in isotropic turbulence," J. Fluid Mech. **67**, 561 (1975).
[24] G. K. Batchelor, *Theory of Homogeneous Turbulence* (Cambridge University Press, Cambridge, 1953).
[25] J. C. Fung, J. C. R. Hunt, N. A. Malik, and R. J. Perkins, "Kinematic simulation of homogeneous turbulent flows generated by unsteady random Fourier modes," J. Fluid Mech. **236**, 281 (1992).
[26] R. Labbé, J.-F. Pinton, and S. Fauve, "Study of the Von Kármán flow between coaxial corotating disks," Phys. Fluids **8**, 914 (1996).
[27] N. Mordant, J.-F. Pinton, and O. Michel, "Time resolved tracking of a sound scatterer in a complex flow: non-stationary signal analysis and applications," J. Acoust. Soc. Am. **112**, 108 (2002).
[28] J.-F. Pinton and R. Labbé, "Correction to the Taylor hypothesis in swirling flows," Phys. Fluids **4**, 1461 (1994).
[29] R. Labbé, J.-F. Pinton, and S. Fauve, "Power fluctuations in turbulent swirling flows," J. Phys. II **6**, 1099 (1996).
[30] E. Inoue, "On turbulent diffusion in the atmosphere," J. Meteorol. Soc. Jpn. **29**, 246 (1951).
[31] S. R. Hanna, "Lagrangian and Eulerian time-scale relations in the daytime boundary layer," J. Appl. Meteorol. **20**, 242 (1981).
[32] S. Du, L. Sawford, J. D. Wilson, and D. J. Wilson, "Estimation of the Kolmogorov constant for the Lagrangian structure-function, using a second-order Lagrangian model grid turbulence," Phys. Fluids **7**, 3083 (1995).
[33] G. Boffetta, A. Celani, A. Crisanti, and A. Vulpiani, "Relative dispersion in fully developed turbulence: Lagrangian statistics in synthetic flows," Europhys. Lett. **46**, 177 (1999).
[34] D. J. Thomson, "Criteria for the selection of stochastic models of particle trajectories in turbulent flows," J. Fluid Mech. **180**, 529 (1987).
[35] H. Kaplan and N. Dinar, "A three-dimensional model for calculating the concentration distribution in inhomogeneous turbulence," Boundary-Layer Meteorol. **62**, 217 (1993).